CPAD 2022
Nov 30th, 2022

THE UNIVERSITY OF NEW MEXICO

Charged Hadron damage investigation of FBK and HPK Low Gain Avalanche Detectors

Jiahe Si, Martin Hoeferkamp, Josef Sorenson, Sally Seidel
University of New Mexico
Gregor Kramberger
Jozef Stefan Institute

Outline

- The High Luminosity (HL) upgrade will increase the luminosity of the Large Hadron Collider (LHC) by a factor of ~10. Increased luminosity causes (1) increased fluence which degrades sensor performance and (2) increased readout complexity because of the pileup.
- Low Gain Avalanche Detectors (LGAD) will be primarily used for fast timing measurement in HL-LHC for the High-Granularity Timing Detector (HGTD) in ATLAS or the Endcap Timing Layer (ETL) of CMS. They are required to operate at a fluence up to 2.5×10^{15} n_{eq}/cm^2 (including a safety factor of 1.5).
- It is required that the HGTD be able to measure the times of arrival of minimum-ionizing particles (MIPs) with an average time resolution of approximately 35 ps per track at the beginning of the operation of the HL-LHC, 70 ps at the end of the operation of the HL-LHC.
- Initial characterization measurements of unirradiated/irradiated LGADs manufactured by Hamamatsu Photonics (HPK) and Fondazione Bruno Kessler (FBK) are underway at UNM.

How do LGADs work?

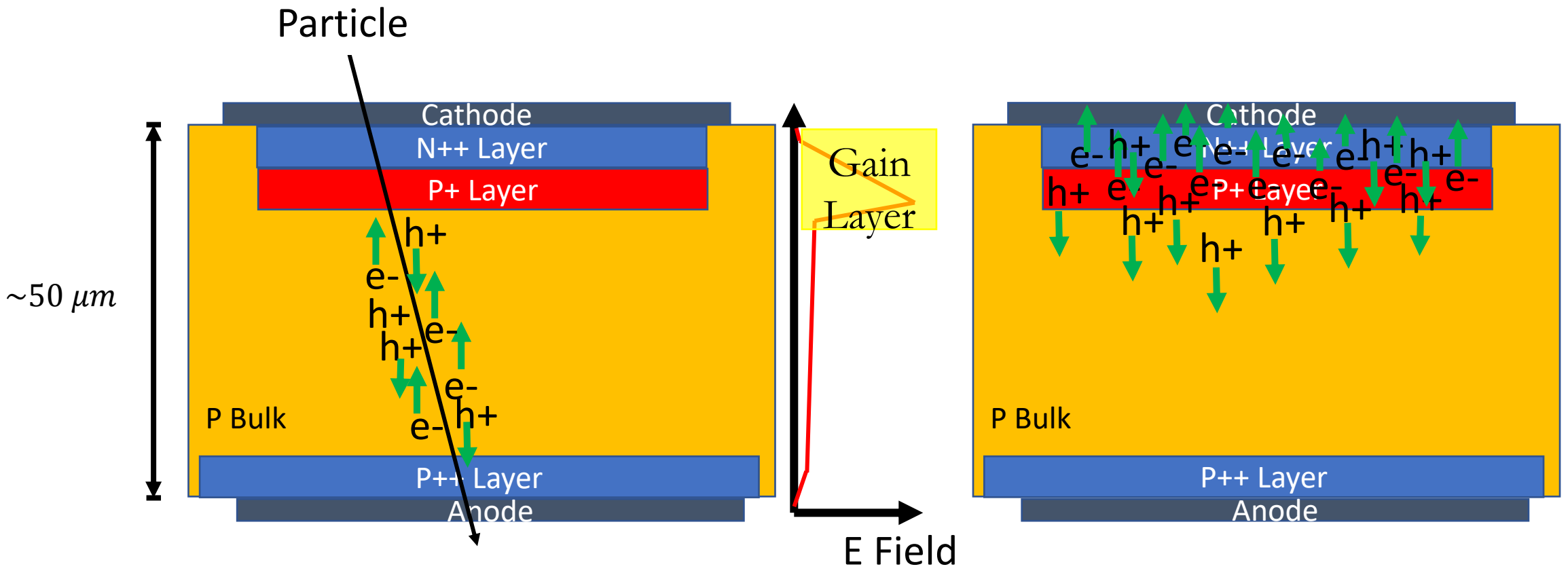

In silicon sensors, charge multiplication happens when charge carriers drift in a region with an electric field (E) greater than about 300 kV/cm. The additional P+ (or gain) layer, when depleted, locally generates an electric field high enough to activate the avalanche process.

Our study includes LGADs manufactured by Hamamatsu Photonics (HPK) and Fondazione Bruno Kessler (FBK).

HPK-P2 Quad Single

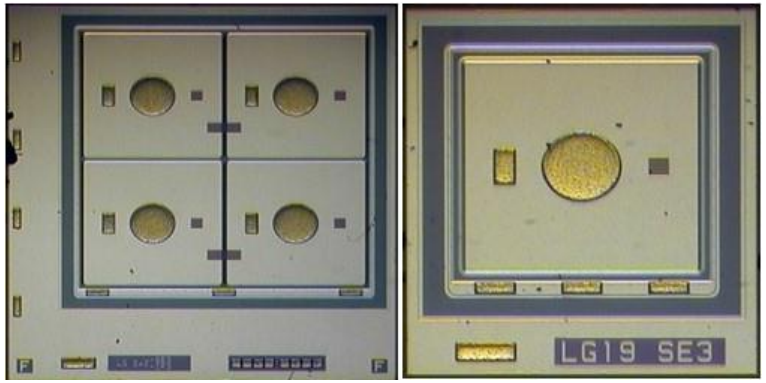

n ++ (electrode) – 1.3 x 1.3 mm^2
p + (gain layer) – 2.2 to 2.5 µm thick
p (bulk)
p ++ (backside)

50 µm thick active layer
200 µm total thickness
single guard ring
variations with and without under-bump metallization (UBM)
epitaxial Si grown on Czochralski substrate

FBK4.0 Double Single Single

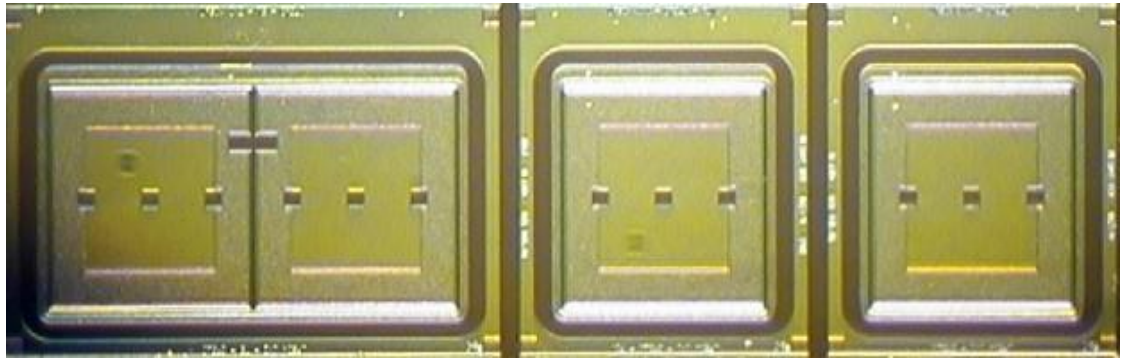

n ++ (electrode) – 1.3 x 1.3 mm^2 Quad Quad
p + (gain layer): 0.7-2µm thick
p (bulk)
p ++ (backside)

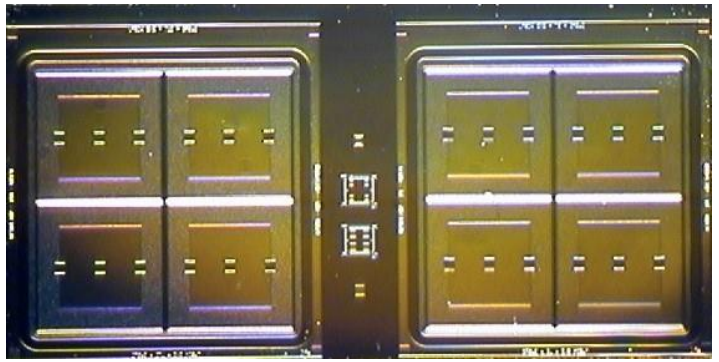

55 µm thick active layer
multiple guard rings
The depth of the gain implant varies in different samples.

In FBK sensors, carbon co-implantation in the gain layer is used to improve radiation resistance. The carbon dose varies in different samples.

LANSCE/FNAL Proton Irradiation

In 2022, we did two irradiation runs. One at Fermi National Accelerator Laboratory (FNAL) in May, and the other one at Los Alamos Neutron Science Center (LANSCE) in July.
Normally at LANSCE we get 800 MeV protons, but in July 2022 run, we irradiated the FBK samples with 500 MeV protons.

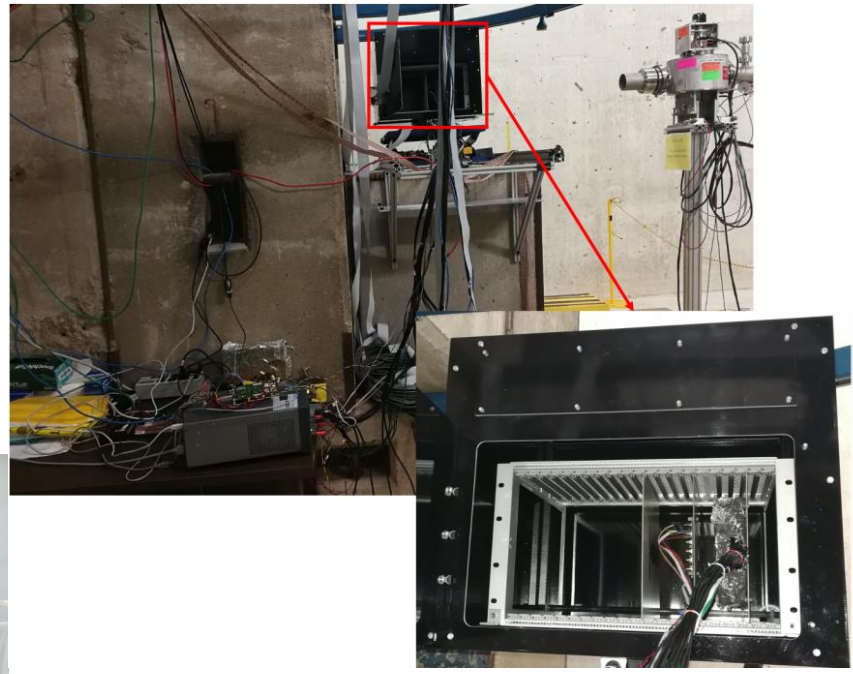

At the FNAL facility, we irradiated HPK samples with 400 MeV protons in May.

Irradiated samples are stored in -25C freezer.

Current vs. Voltage (IV) measurements are used to measure leakage currents, breakdown voltages, and determine the operational ranges.

Keithley 237 source meter provides bias voltage and reads out the leakage current.

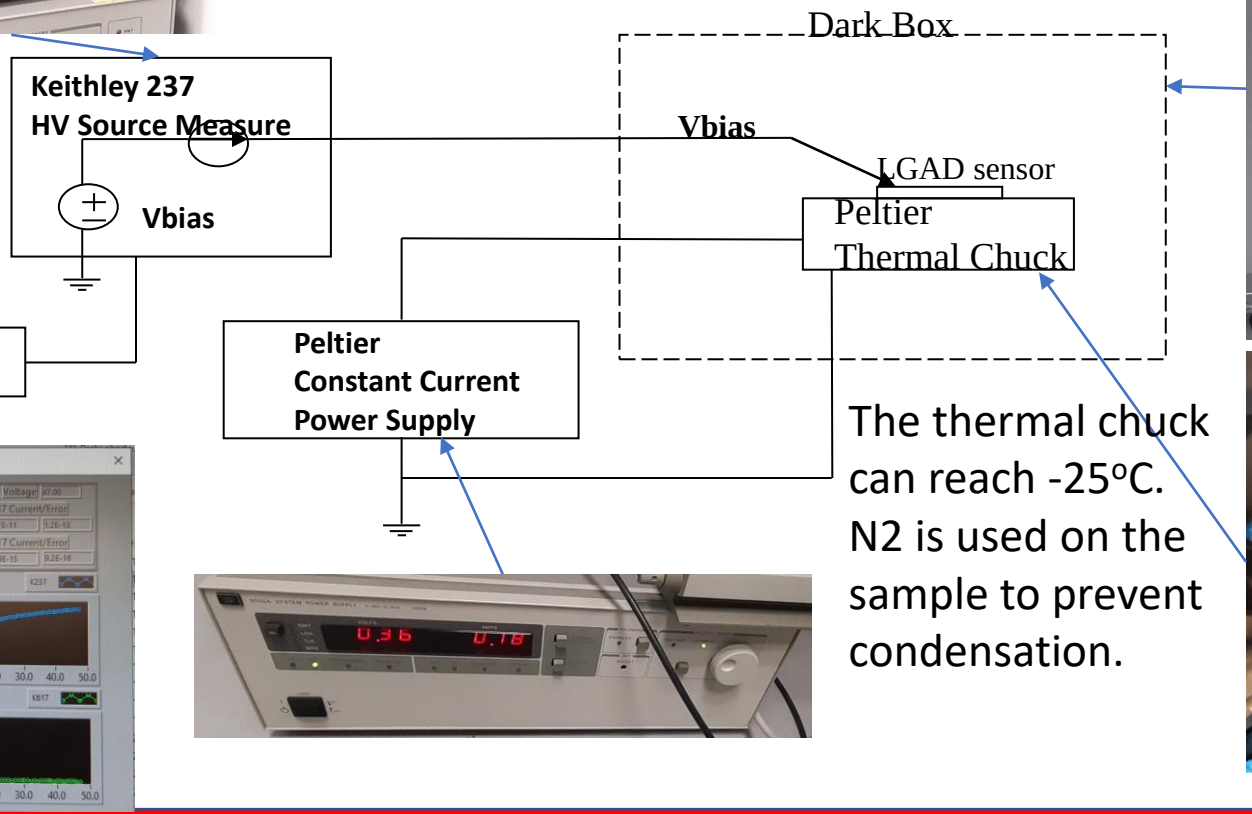

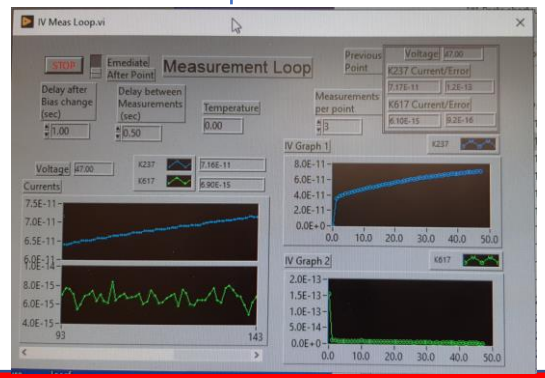

The thermal chuck can reach -25°C. N2 is used on the sample to prevent condensation.

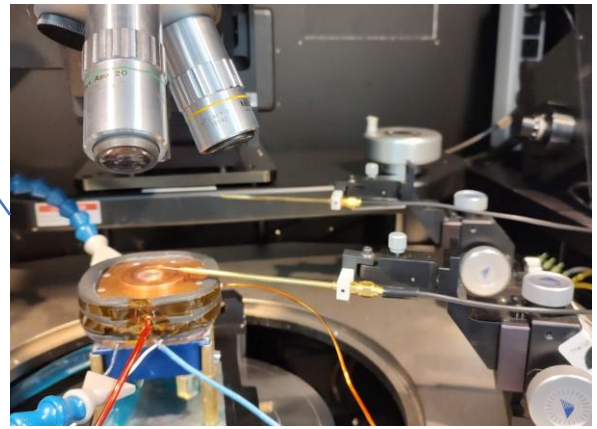

Irradiation increases leakage currents and breakdown voltages of LGADS

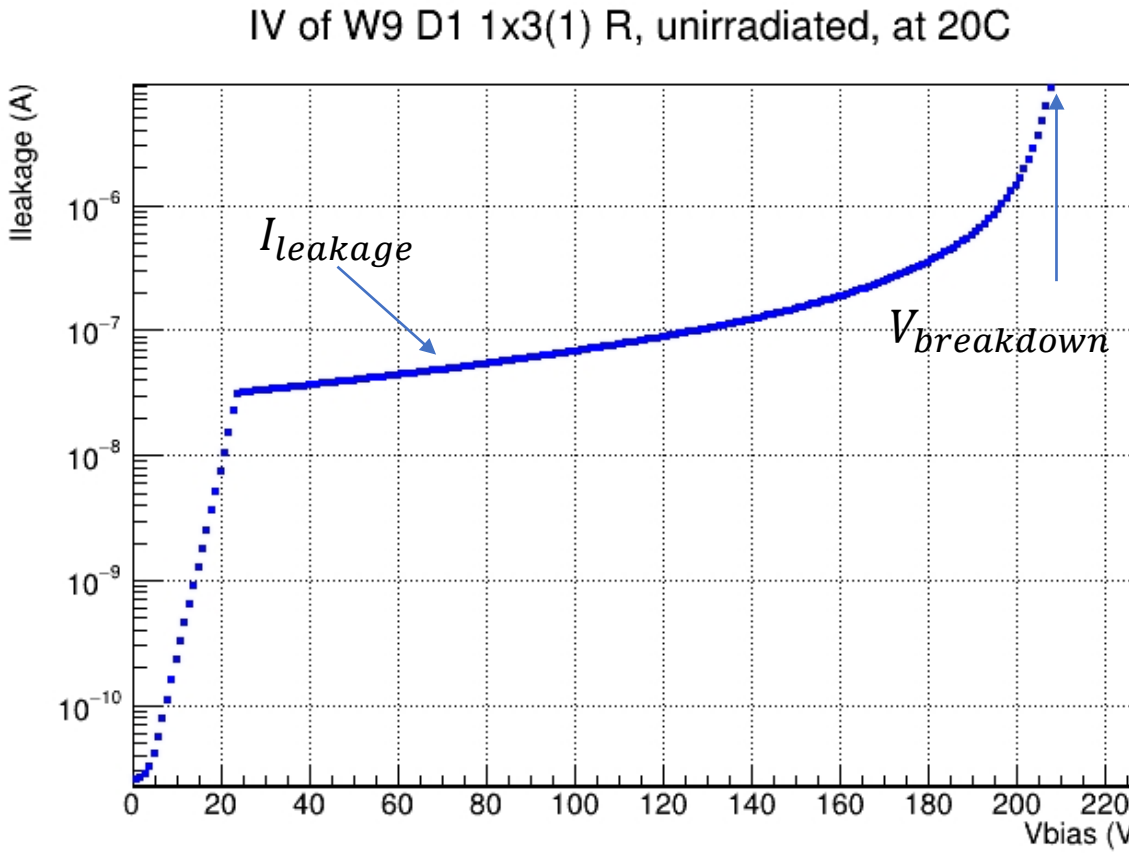

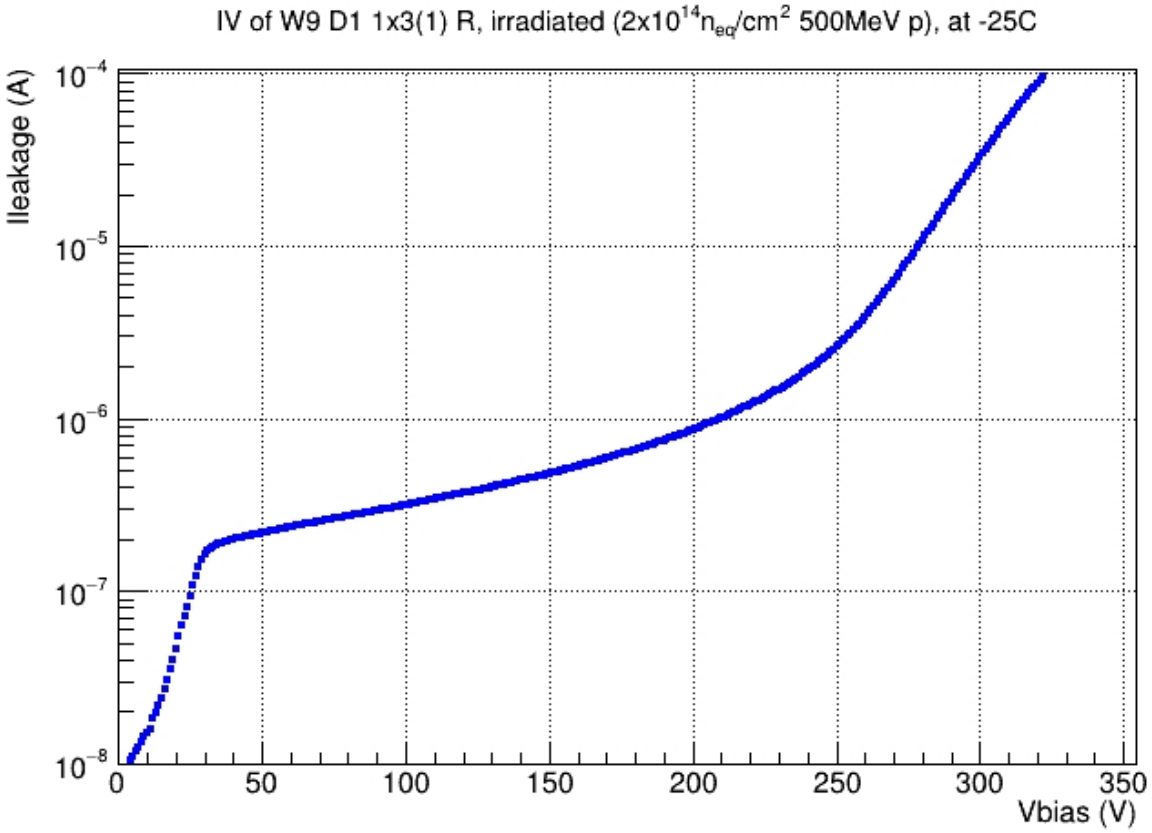

Capacitance vs. Voltage (CV) Measurements are used to measure the depletion voltage

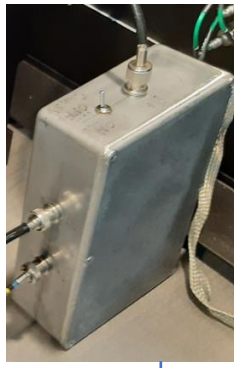

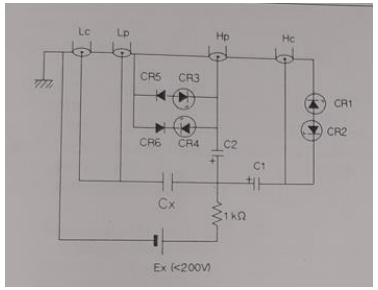

Keithley 237
HV Source
Measure

Vbias

HP4284A
LCR Meter

Bias
Isolation
Box

Dark Box

Vbias

LGAD sensor

Peltier
Thermal Chuck

PC with LabView

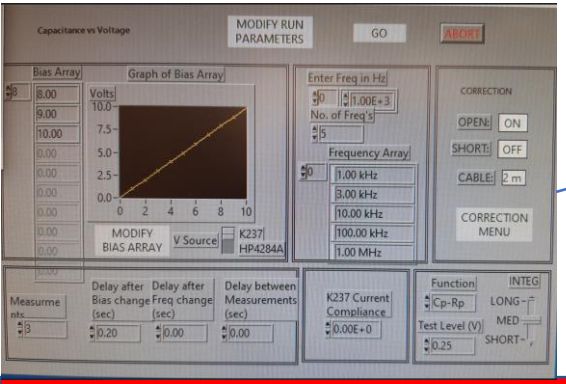

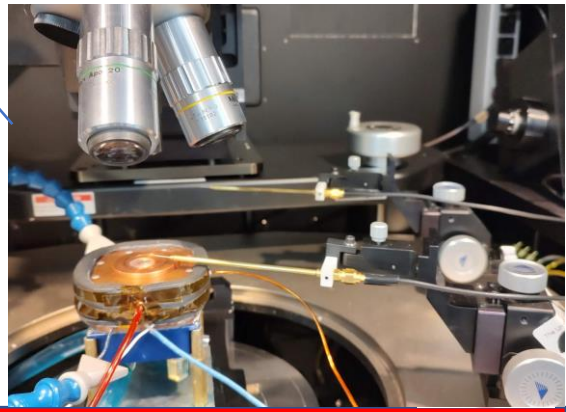

CV Measurements are used to extract the gain layer depletion voltage V_{gl} and full depletion voltage V_{fd}

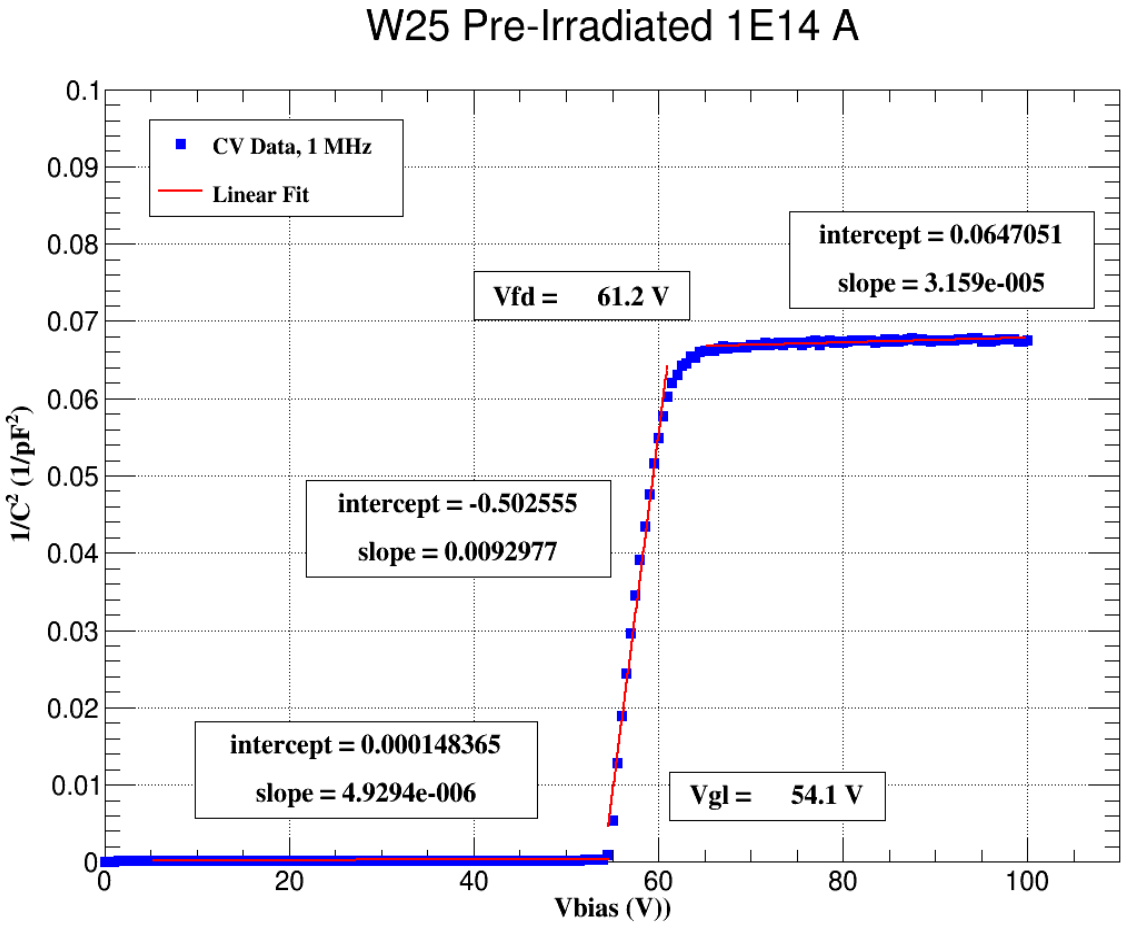

The depletion voltage of the gain layer depends on the dopant concentration, which is impacted by radiation fluence

Dopant Concentration

Electron charge

Gain Layer depth

Gain layer depletion voltage

$$V_{gl} = \frac{qN_A w^2}{2\epsilon}(1+2\frac{d}{w})$$

Permittivity of Silicon

Gain Layer Thickness

β-source setup is used to study the timing performance of LGADs

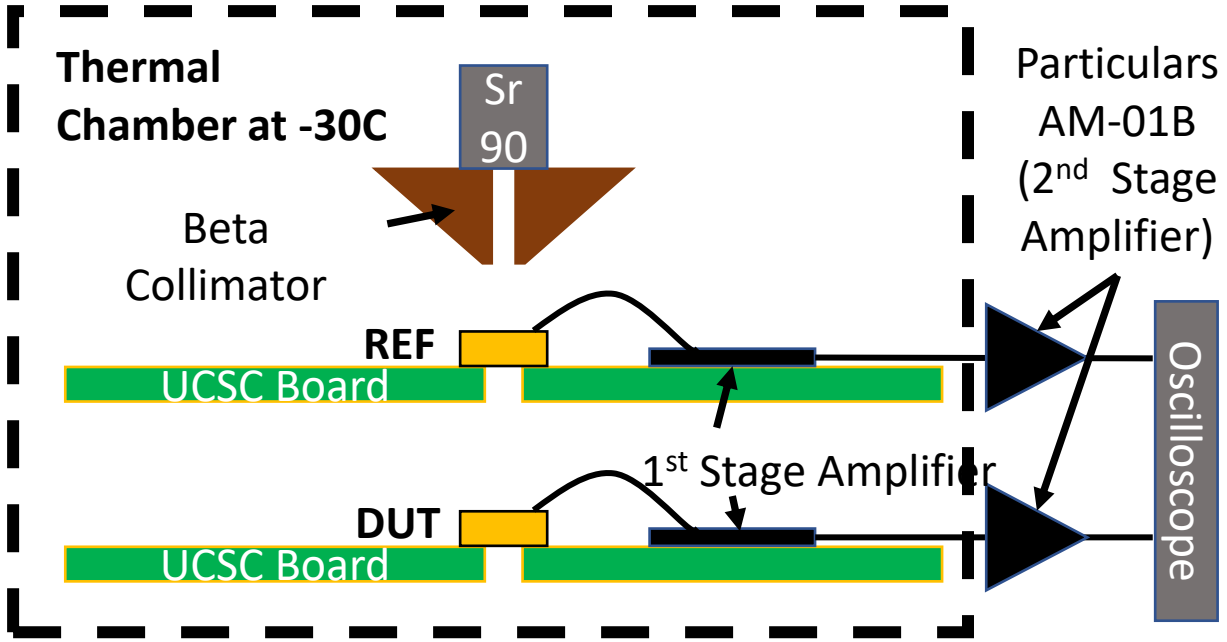

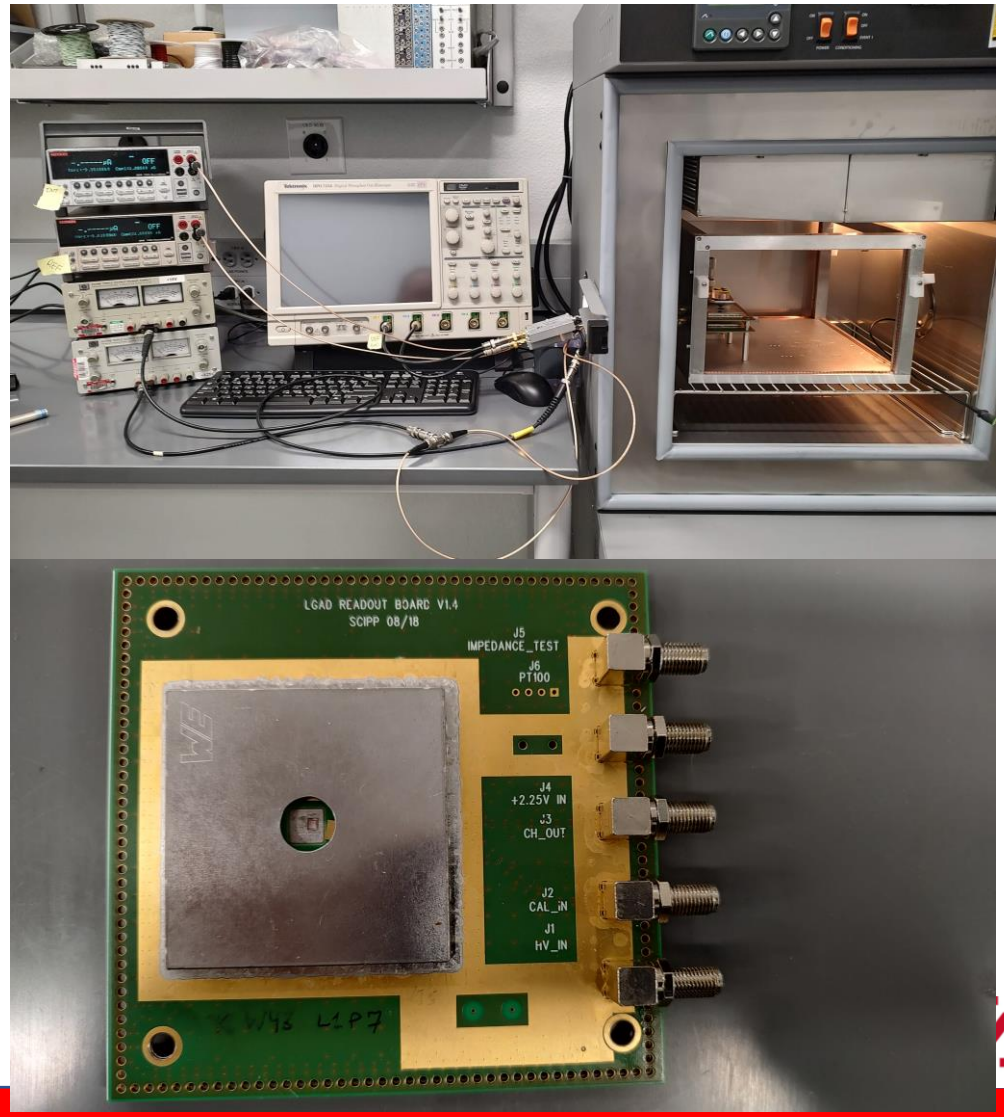

- LGADs are mounted on the single channel readout board developed by UCSC.
- Tektronix DPO 7254 Oscilloscope with 2.5GHz bandwidth, 40GS/s sampling rate is used.
- Shortest cables are used to connect to the oscilloscope for best signal-to-noise performance.
- Time resolution requirement: 35 ps (start) and 70 ps (end of life).

3 methods were used to calculate the resolution

- Only signals triggering both REF and DUT channels are collected.
- The resolution is calculated from the temporal deviation of ~2000 events.
- Constant Fraction Discriminator (CFD) method of 25%, 2-point linear fitting, and 4-point linear fitting were used, the differences are within a few percent.
- Equation $\sigma_{tot}^2 = \sigma_{REF}^2 + \sigma_{DUT}^2$ is used to calculate the resolution.

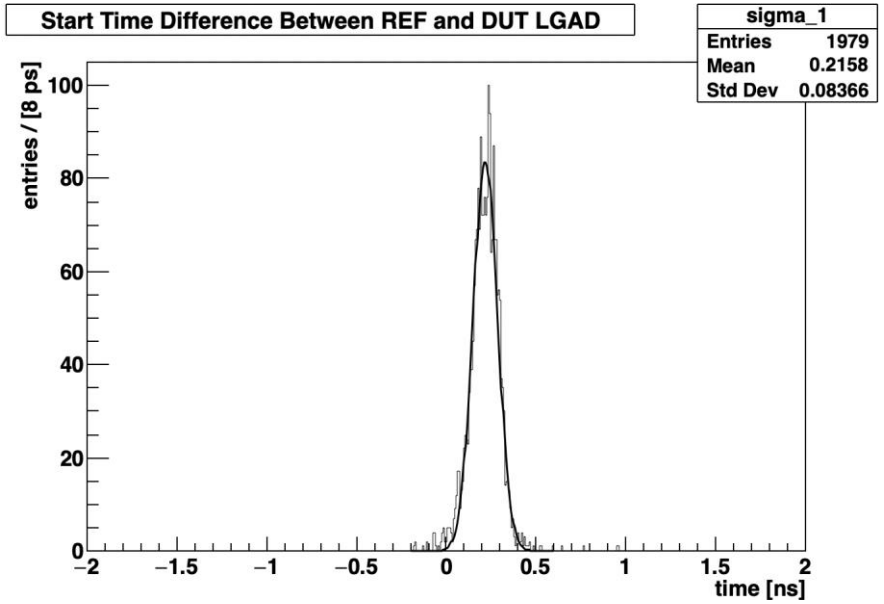

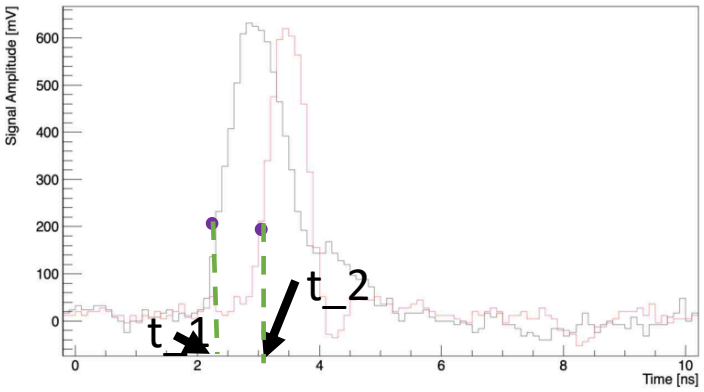

CFD of 25%

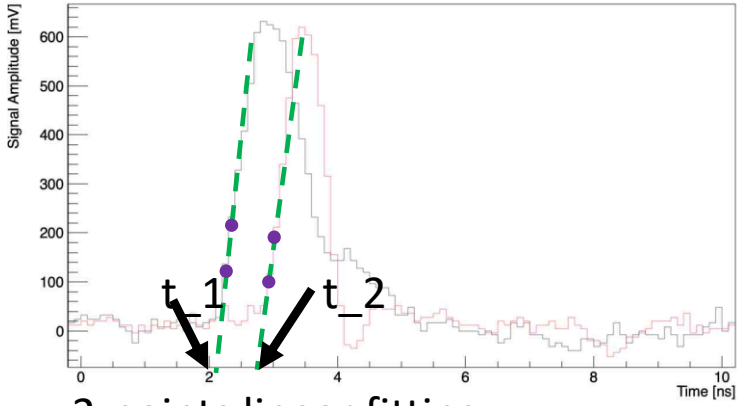

2-points linear fitting

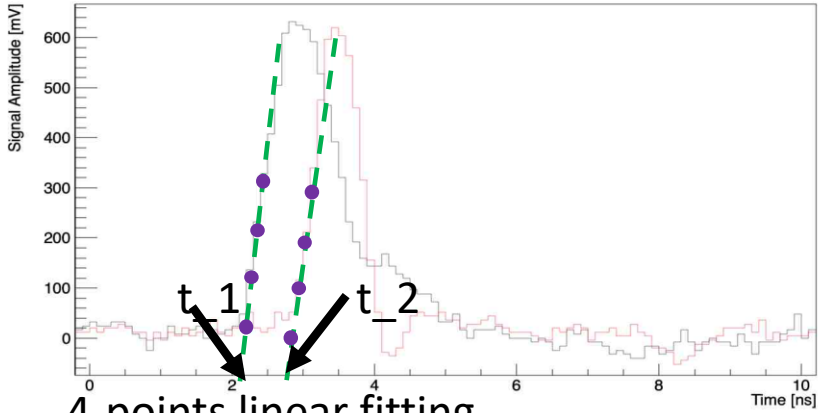

4-points linear fitting

Two identical HPK sensors (unirradiated) are used as the references for timing measurements

When measuring the timing of two identical sensors, $\sigma_{REF} = \sigma_{DUT}$ so a single measurement will give you the temporal resolution of both sensors.

Either of the unirradiated sensors can be used as the reference for the timing measurements for the irradiated sensors.

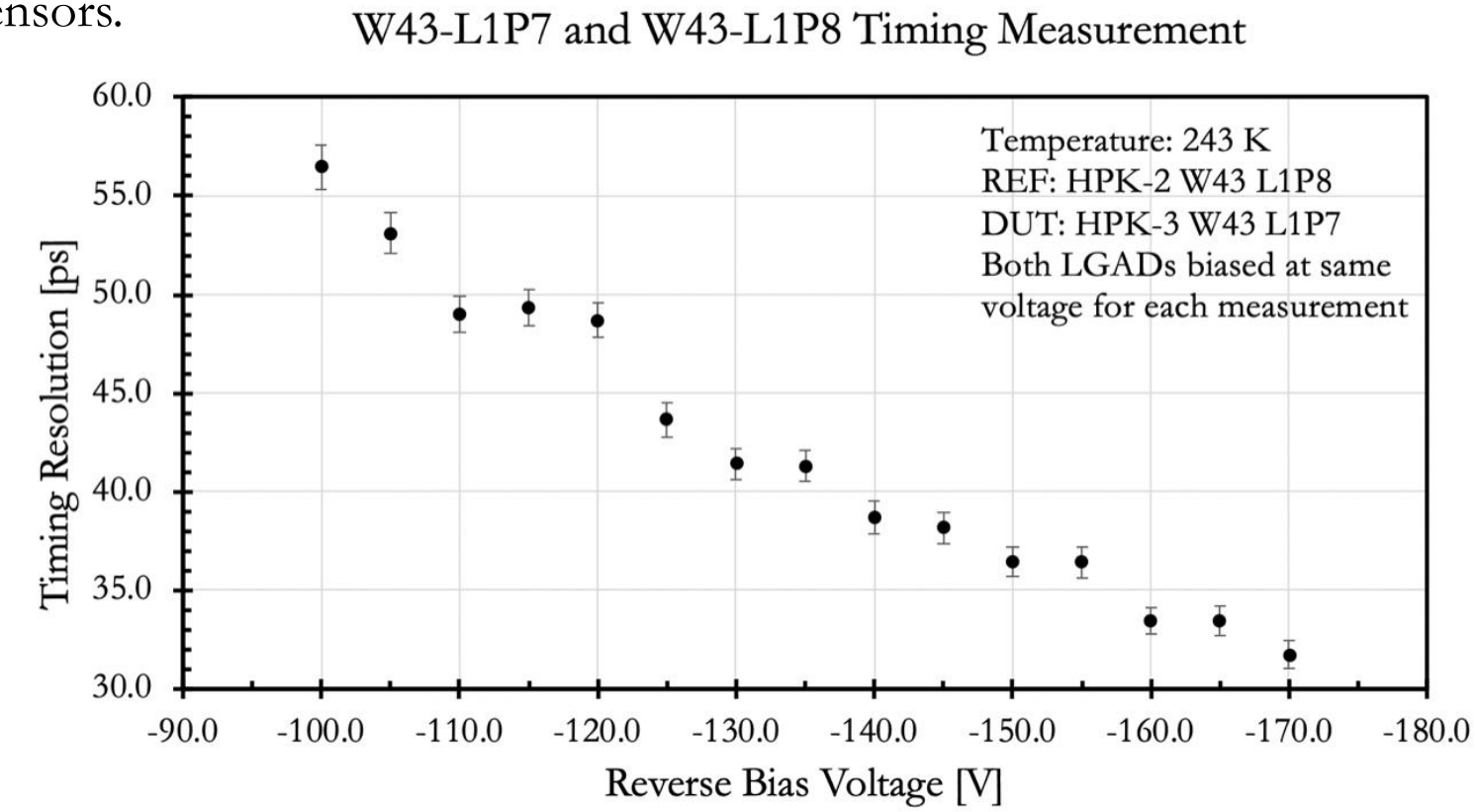

Study of the effect of high temperature annealing upon LGAD capacitance and current

To match the LGAD community's standard procedure, irradiated samples were annealed at 60°C for 80 minutes. However, pre-annealing measurements were also performed.

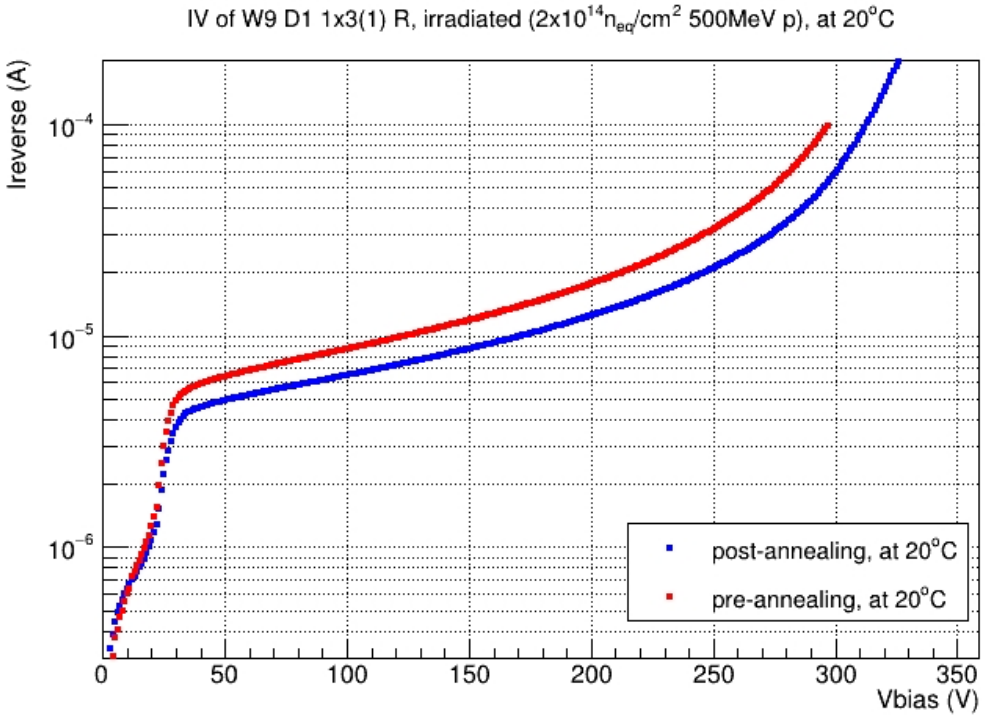

After annealing, leakage current reduced by ~1/3, Breakdown voltage increased ~20V.

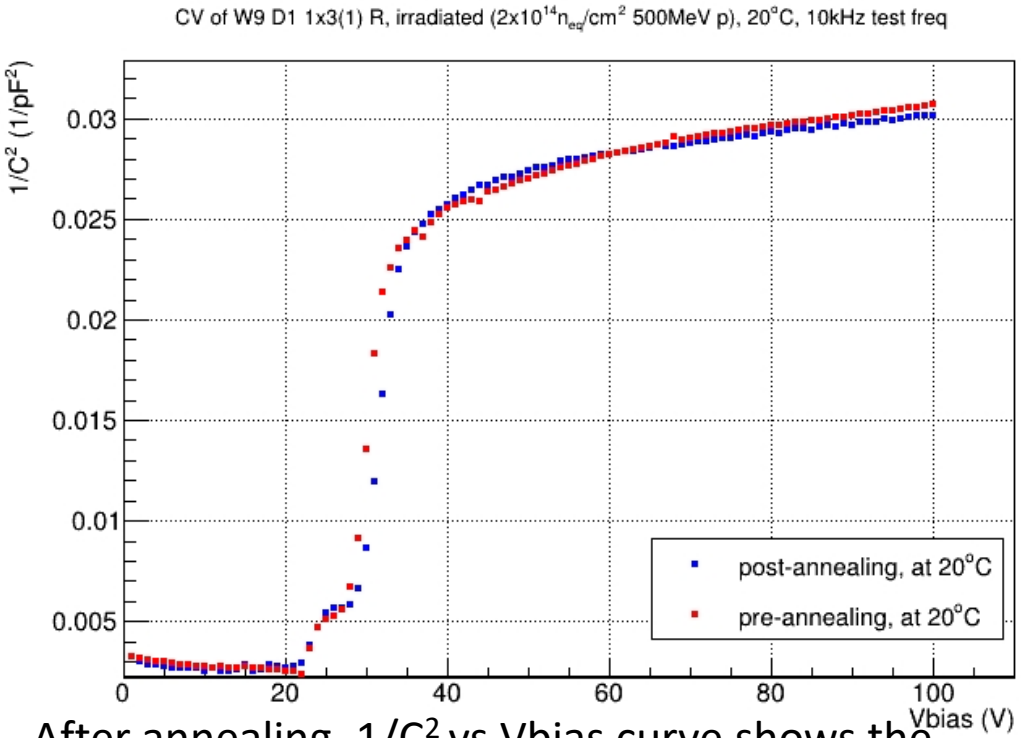

After annealing, $1/C^2$ vs Vbias curve shows the concentration has a mild change. Understanding CV characteristics of irradiated sensors is our next goal…

Preliminary timing resolution measurement is ongoing…

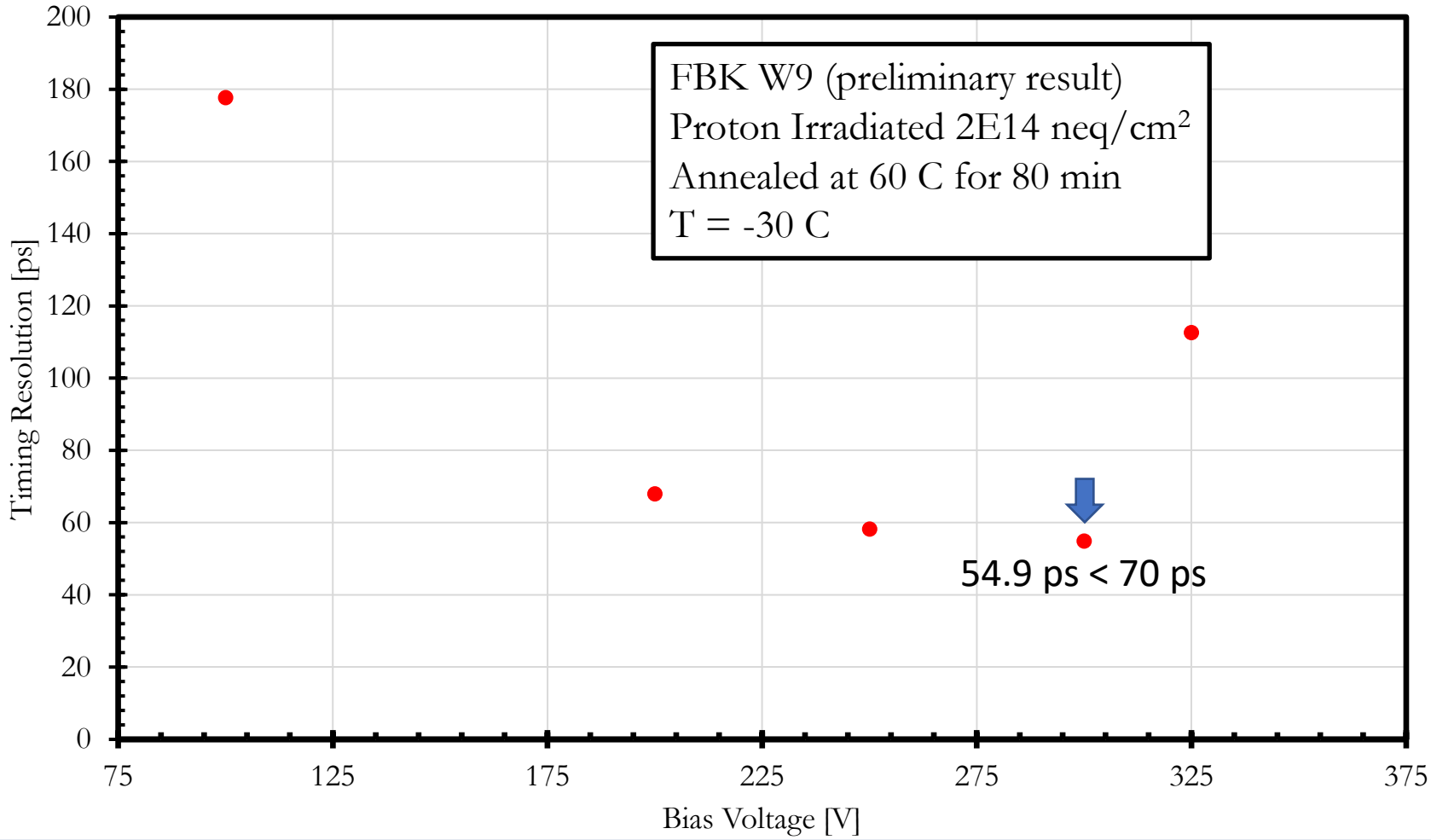

Summary

- We have set up the instruments for IV, CV, and timing measurement.
- Two irradiation runs were performed at FNAL and LANSCE in 2022.
- Pre-irradiation measurements were performed.
- Working on post-irradiation measurements (just started).
- With the LGADs irradiated at different fluences, one of our goals is to estimate acceptor removal coefficients using $V_{gl} = \frac{qN_A w^2}{2\epsilon}(1+2\frac{d}{w})$
- There are still many samples to measure and study…

Thank You!

Backup Slides

From Technical Design Report:
A High-Granularity Timing Detector for the
ATLAS Phase-II Upgrade p88
ATLAS-TDR-031.pdf

Technology	Silicon Low Gain Avalanche Detector (LGAD)
Time resolution	≈ 35 ps (start); ≈ 70 ps (end of lifetime)
Time resolution uniformity	No requirement
Min. gain	20 (start); 8 (end of lifetime)
Min. charge	4 fC
Min. hit efficiency	95%
Granularity	1.3 mm $\times$ 1.3 mm
Max. inter-pad gap	100 µm
Max. physical thickness	300 µm
Active thickness	50 µm
Active size	39 mm $\times$ 19.5 mm (30 $\times$ 15 pads)
Max. inactive edge	500 µm
Radiation tolerance	2.5×10^{15} n_{eq} cm^{-2}, 1.5 MGy
Max. operation temperature on-sensor	-30 °C
Max. leakage current per pad	5 µA
Max. bias voltage	800 V
Max. power density	100 mW/cm^2

Table 5.1: Sensor parameters and requirements.

From Technical Design Report:
A High-Granularity Timing Detector for the
ATLAS Phase-II Upgrade p110
ATLAS-TDR-031.pdf

Annealing

Most of the measurements with irradiated sensors were done after annealing for 80 min at 60 °C, which roughly simulates the operational conditions in one year of LHC operation since higher temperature accelerates the annealing (the Arrhenius factor between 60 °C and −30 °C is more than 1×10^6, 80 min simulates hundreds of years at −30 °C, and tens of days at room temperature).

The actual design includes p-stops to limit inter-pad current, guard rings, and junction termination extensions which mitigate breakdown voltage, and other features.

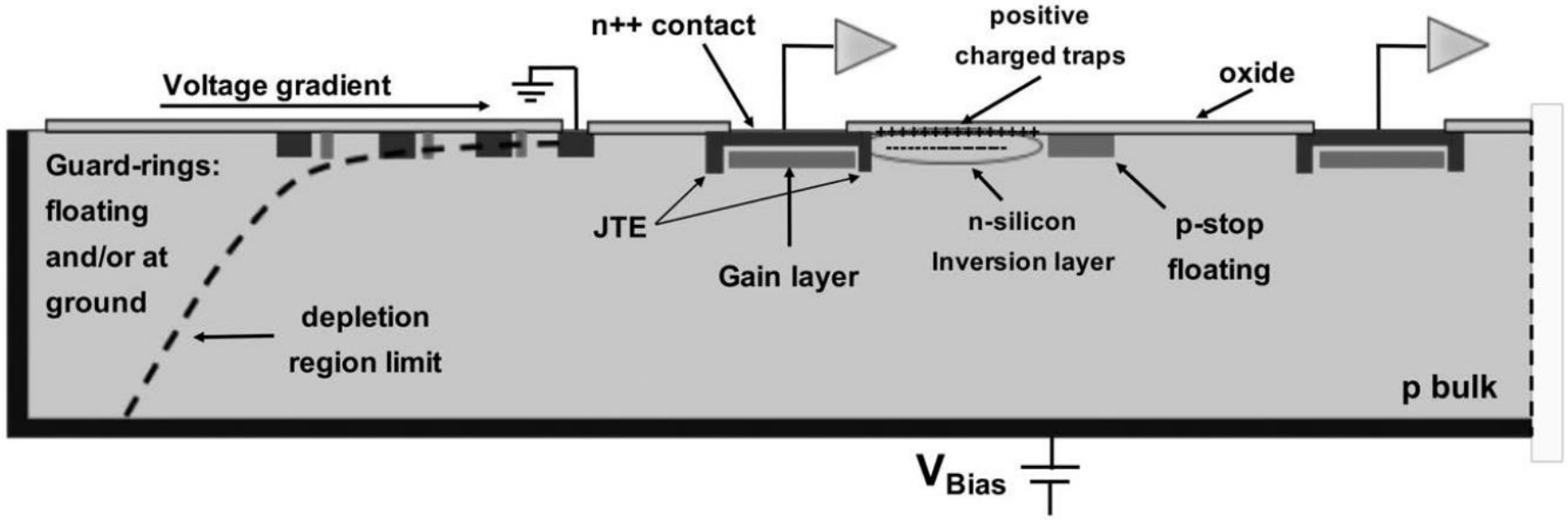

Figure 2.21 Cross cut of a multi-pads UFSD (not to scale) with a schematic view of the building blocks of the device. From the device physical edge: guard-rings, pad with JTEs, inter-pad region with *p*-stop.

An Introduction to Ultra-Fast Silicon Detectors p33

An Introduction to Ultra-Fast Silicon Detectors p84

Using the information provided by the $C(V)$ measurements, it is possible to:

1. extract the gain layer implant profile (amplitude, width, depth) by computing the active doping concentration $N_A(d)$ as a function of depth d. This is obtained by first calculating d from the value of C with

$$d = \frac{\varepsilon_{Si} A}{C} \tag{4.4}$$

and then the doping density at that depth d with:

$$N_A = \frac{2}{\varepsilon_{Si} q A^2 \frac{\partial 1/C^2}{\partial V}}, \tag{4.5}$$

An Introduction to Ultra-Fast Silicon Detectors p38

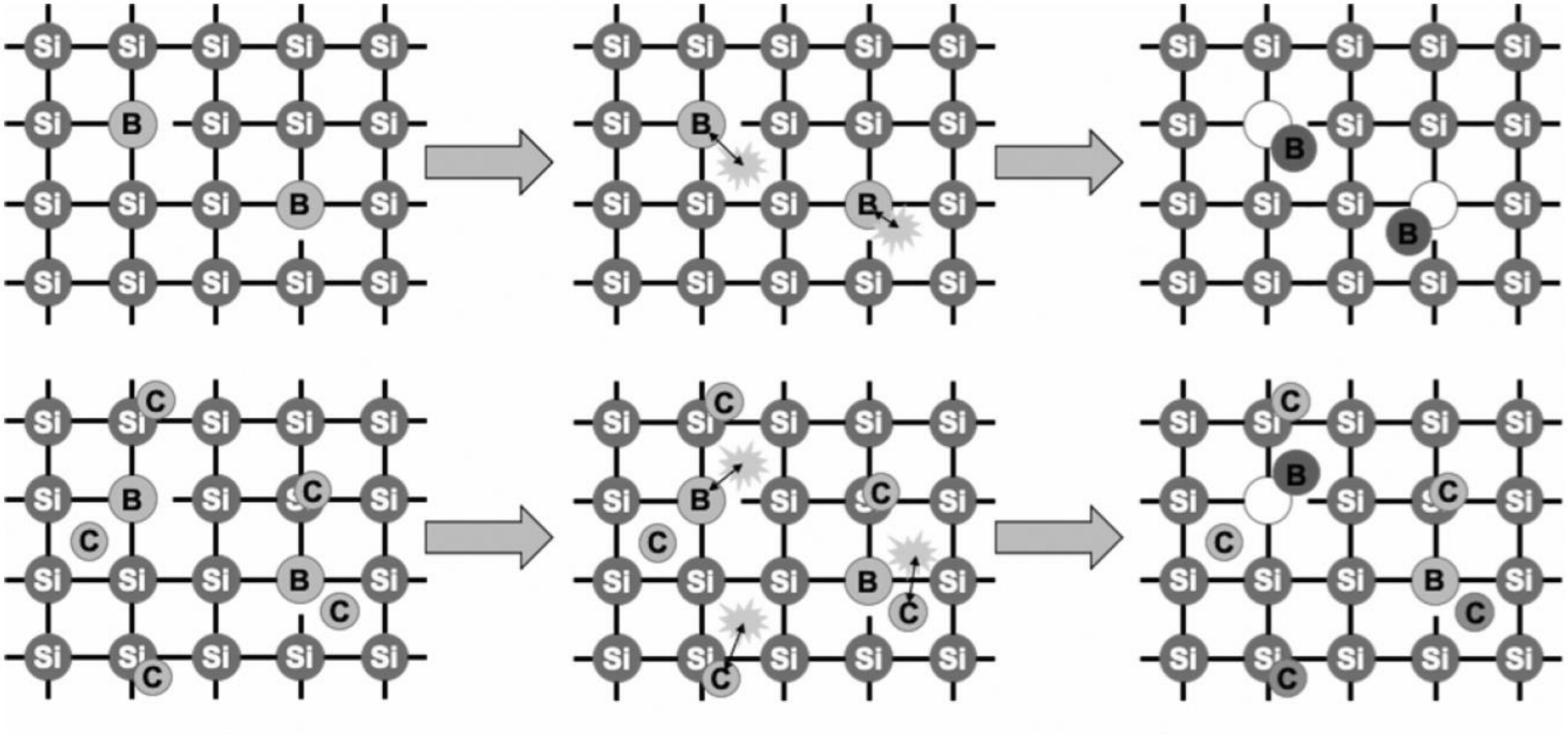

An Introduction to Ultra-Fast Silicon Detectors p16

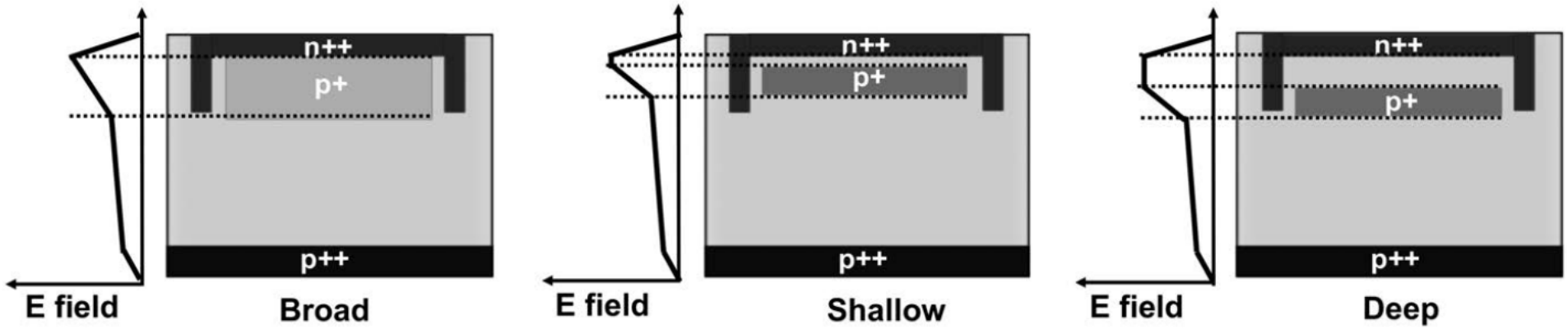

Figure 2.3 Schematic cross cut of a UFSD with broad (*left*), shallow (*middle*), and deep (*right*) gain implants and their respective electric field profiles.

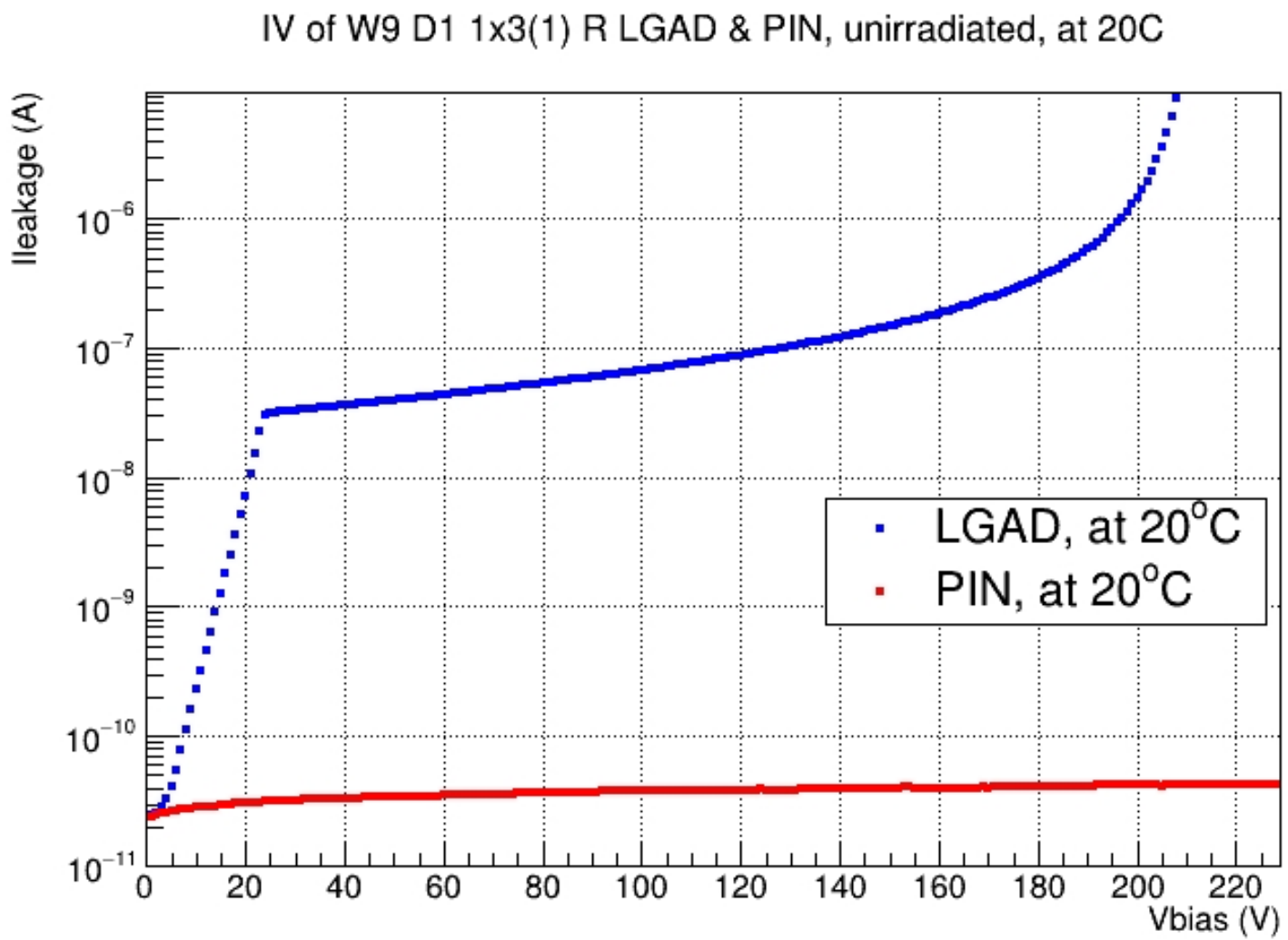
IV of W9 D1 1x3(1) R LGAD & PIN, unirradiated, at 20C
Ileakage (A)
10^{-6}
10^{-7}
10^{-8}
10^{-9}
10^{-10}
10^{-11}
0
20
40
60
80
100
120
140
160
180
200
220
Vbias (V)
LGAD, at 20°C
PIN, at 20°C